

See discussions, stats, and author profiles for this publication at: <https://www.researchgate.net/publication/260152460>

A New Electrochemical Approach for the Synthesis of Copper–Graphene Nanocomposite Foils with High Hardness

Article in *Scientific Reports* · February 2014

DOI: 10.1038/srep04049 · Source: PubMed

CITATIONS

207

READS

1,825

5 authors, including:



Sarada Bulusu

International Advanced Research Centre for Powder Metallurgy and New Materials

70 PUBLICATIONS 2,853 CITATIONS

[SEE PROFILE](#)



Koteswararao V. Rajulapati

University of Hyderabad

67 PUBLICATIONS 994 CITATIONS

[SEE PROFILE](#)



Govindan Sundararajan

Indian Institute of Technology Madras

128 PUBLICATIONS 4,310 CITATIONS

[SEE PROFILE](#)

Some of the authors of this publication are also working on these related projects:



solar cells [View project](#)



Lithium ion battery for EV application [View project](#)



OPEN

SUBJECT AREAS:

MECHANICAL AND
STRUCTURAL PROPERTIES
AND DEVICESELECTRONIC MATERIALS
SYNTHESIS AND PROCESSING

A New Electrochemical Approach for the Synthesis of Copper-Graphene Nanocomposite Foils with High Hardness

Chokkakula L. P. Pavithra^{1,2}, Bulusu V. Sarada¹, Koteswararao V. Rajulapati², Tata N. Rao¹ & G. Sundararajan¹

Received

6 November 2013

Accepted

14 January 2014

Published

11 February 2014

Correspondence and
requests for materials
should be addressed to
B.V.S. (sarada@arci.
res.in)¹International Advanced Research Centre for Powder Metallurgy and New Materials (ARCI), Balapur (PO), Hyderabad, 500005, INDIA. ²School of Engineering Sciences and Technology (SEST), University of Hyderabad, Gachibowli, Hyderabad, 500046, INDIA.

Graphene has proved its significant role as a reinforcement material in improving the strength of polymers as well as metal matrix composites due to its excellent mechanical properties. In addition, graphene is also shown to block dislocation motion in a nanolayered metal-graphene composites resulting in ultra high strength. In the present paper, we demonstrate the synthesis of very hard Cu-Graphene composite foils by a simple, scalable and economical pulse reverse electrodeposition method with a well designed pulse profile. Optimization of pulse parameters and current density resulted in composite foils with well dispersed graphene, exhibiting a high hardness of ~ 2.5 GPa and an increased elastic modulus of ~ 137 GPa while exhibiting an electrical conductivity comparable to that of pure Cu. The pulse parameters are designed in such a way to have finer grain size of Cu matrix as well as uniform dispersion of graphene throughout the matrix, contributing to high hardness and modulus. Annealing of these nanocomposite foils at 300°C , neither causes grain growth of the Cu matrix nor deteriorates the mechanical properties, indicating the role of graphene as an excellent reinforcement material as well as a grain growth inhibitor.

The extremely superior properties of the recently emerged material, graphene (Gr), consisting of a single to few layers of covalently bonded sp^2 carbon atoms, hexagonally packed in a honeycomb crystal lattice, allow it to surpass CNTs as an ideal reinforcement into the matrix material^{1,2}. Gr exhibits exceptional mechanical properties (Young's modulus of ~ 1 TPa and tensile strength of ~ 130 GPa)³, good electrical conductivity⁴ and better thermal properties ($K \sim 5000 \text{ W m}^{-1} \text{ K}^{-1}$)⁵. Owing to its two dimensional sheet-like structure with high aspect ratio and large surface area compared to CNTs, Gr is expected to enhance the properties of the composites². Unlike CNTs, Gr can be prepared in large quantities by inexpensive methods by chemical and electrochemical exfoliation of graphite^{6,7}. Copper (Cu) matrix nanocomposites have witnessed an enormous growth during the past decade, due to their enhanced mechanical, electrical and thermal properties leading to numerous electronic applications. The conventionally used reinforcements in the Cu matrix such as oxides⁸, carbide nanoparticles etc.⁹, have resulted in considerable improvement in the mechanical properties. However, because of their poor electrical conductivity, they are not desirable for electronic applications. Therefore, carbon as a reinforcement material, in the form of fibres, nanotubes etc.¹⁰, has garnered the attention of scientific community due to the exhibition of superior mechanical, electrical properties and an extremely high thermal conductivity simultaneously¹¹. The demand for a superior material with enhanced mechanical and electrical properties for the electronics industry has led to the development of Cu-CNT composites by different methods^{12,13}. However, the commercialisation of CNT reinforced composites is hampered by the challenges to overcome the agglomeration of CNTs and impurities associated with them, in addition to high production cost. Moreover the tubular structure and high aspect ratio of CNTs led to entanglement that in turn resulted in rough and porous nanocomposites^{14,15}.

Koratkar's research group, for the first time, has shown that a low nanofiller content of Gr in the polymer matrix exhibits a better performance over those with CNTs in terms of mechanical properties¹⁶. Several other researchers have also reported an enhancement in the mechanical¹⁷, thermal¹⁸ and electrical properties¹⁹ of polymer based composites with small amounts of Gr introduced into the matrix. Walker et al.²⁰ have shown a



significant improvement of 235% in the toughness for a Si_3N_4 -Gr nanocomposite compared to its bare counterpart. However, very limited research investigations on metal matrix composites with Gr and Graphene Oxide (GO) as the filler materials are available. With the addition of Gr into $\text{Al}^{21,22}$ and Mg^{23} matrices by powder metallurgy routes, into Ni^{24} by Direct Current (DC) electrodeposition and into Cu^{25} by a molecular mixing process, improvement in mechanical properties of the respective composites was witnessed. Tatyana et al.²⁶ have reported a 39% increment in hardness of Cu-Gr composite prepared via the powder metallurgy route. Hwang et al.²⁵, achieved a 30% enhancement in elastic modulus and 80% improvement in the yield strength, for Cu-Gr composites, in comparison to pure Cu. The electrical resistivity of these composites is also reported to be in the same order as that of pure Cu. Jagannadham has shown an improvement in the thermal conductivity up to 460 W/m-K^{27} , and an electrical resistivity of $2 \times 10^{-6} \Omega \text{ cm}^{28}$ for Cu-Gr composites prepared by DC electrodeposition. Recently Kim et al.²⁹, demonstrated ultra-high strength of 1.5 GPa for Cu-Gr composite nanopillars by designing alternating layers of Cu and monolayered Gr with 70 nm repeat layer spacings, thereby indicating the possibility of achieving high strength even in practical processes such as electroplating by introducing homogeneous distribution of Gr into Cu matrix. The electrodeposition technique, especially with application of pulsed currents is an easy, cost effective and scalable method to incorporate filler materials with nano-sized dimensions homogeneously throughout the matrix³⁰. In addition, electrodeposition being a low temperature process, preserves the properties of Gr and GO during the preparation of the composites unlike in the conventional sintering processes, which could destruct Gr/GO since they may involve temperatures higher than the decomposition temperature of Gr/GO ($>600^\circ\text{C}$)²⁵. To the best of our knowledge, there are no reports on Cu-Gr composites prepared by pulse reverse

electrodeposition (PRED) with enhanced mechanical properties while retaining the electrical properties similar to that of pure Cu.

In the present paper, for the first time, we report the preparation of Cu-Gr composite foils by PRED with a hardness of $\sim 2.5 \text{ GPa}$ and an elastic modulus of $\sim 137 \text{ GPa}$, which are about ~ 2 times and 1.2 times higher, respectively, compared to those of bulk Cu (Hardness and Elastic modulus of bulk Cu are 1.2 GPa and 116 GPa, respectively) while maintaining the electrical resistivity in the same range³¹. PRED facilitates a uniform distribution of Gr sheets into the Cu matrix, where they spread around the grains through grain boundaries to achieve an improved interface with Cu throughout the sheet. Electrochemically exfoliated Graphene Oxide (GO)⁶ is used in the present work as it is easy to disperse uniformly in the electrolyte due to the presence of oxygen containing functional groups, as confirmed by FTIR (Figure S2 Supporting information). The advantage of electrochemical exfoliation is that it minimizes the damage to the GO sheet⁶ during exfoliation unlike in the case of harsh chemical methods. For preparing the Cu-Gr composite foils, GO concentration in the electrolyte was varied between 0.1–1.0 gm/L. GO concentration of 0.5 gm/L in the electrolyte resulted in Cu-Gr foils with the best mechanical properties of the composite. Subsequently, these foils were annealed under argon atmosphere at 300°C for 30 minutes in order to reduce GO to Gr. It is also plausible that GO in the Cu matrix could partially reduce to Gr during the electrodeposition because of application of large cathodic pulses during the deposition process. It has been reported that Gr and GO exhibit hardness and modulus in the same range, where GO shows a slightly lower hardness³². Figure 1 (a–e) represents the schematic of the electrodeposition process employed in the current investigation. Full details of the deposition process are discussed in the experimental methods section.

Figures 2(a) & 2(b) show the Transmission Electron Microscopic (TEM) images of the electrochemically exfoliated GO nanosheets.

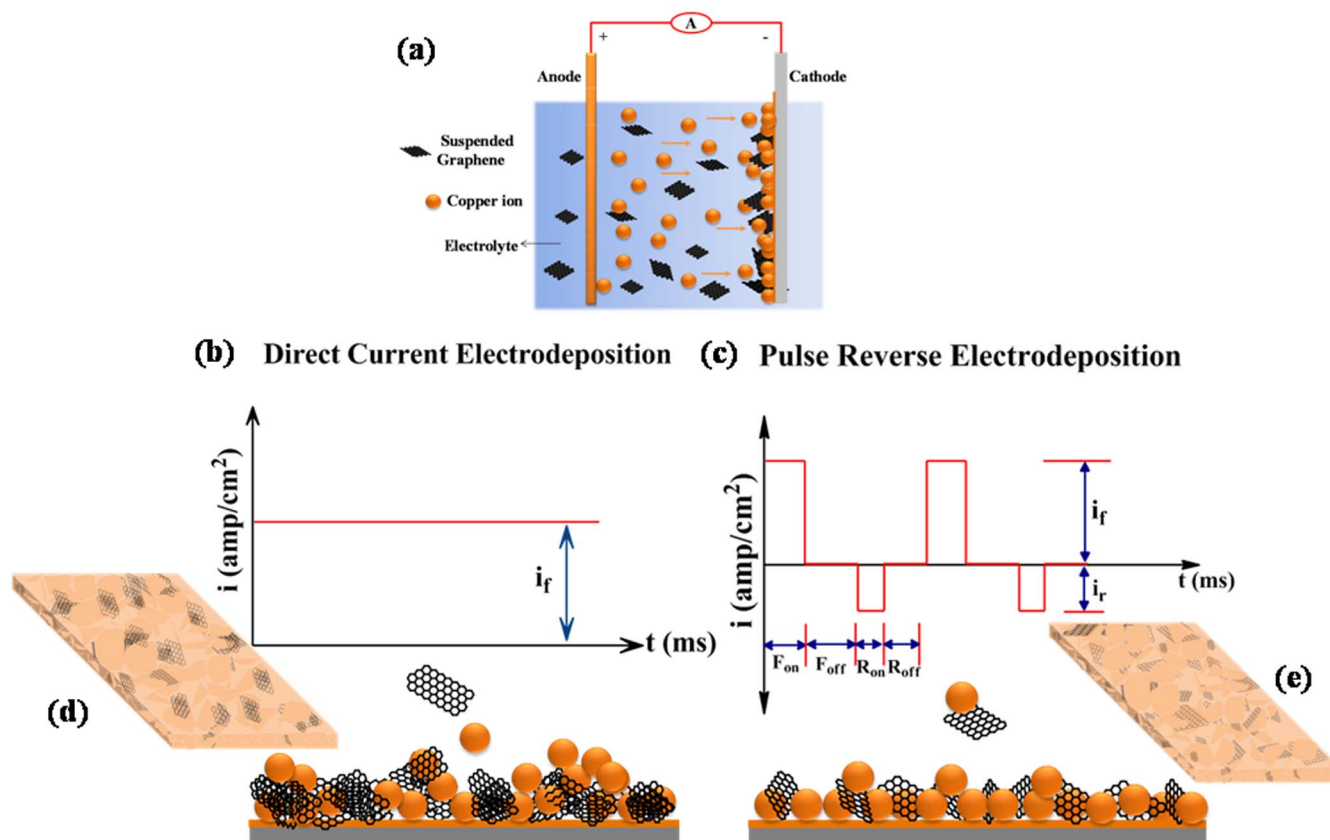


Figure 1 | (a) Experimental setup of electrodeposition, (b)&(c) Schematic representation of the current waveforms and the co-deposition of Cu and Gr, (d) & (e) Cu-Gr nanocomposite foils prepared by DC and PRED, respectively.

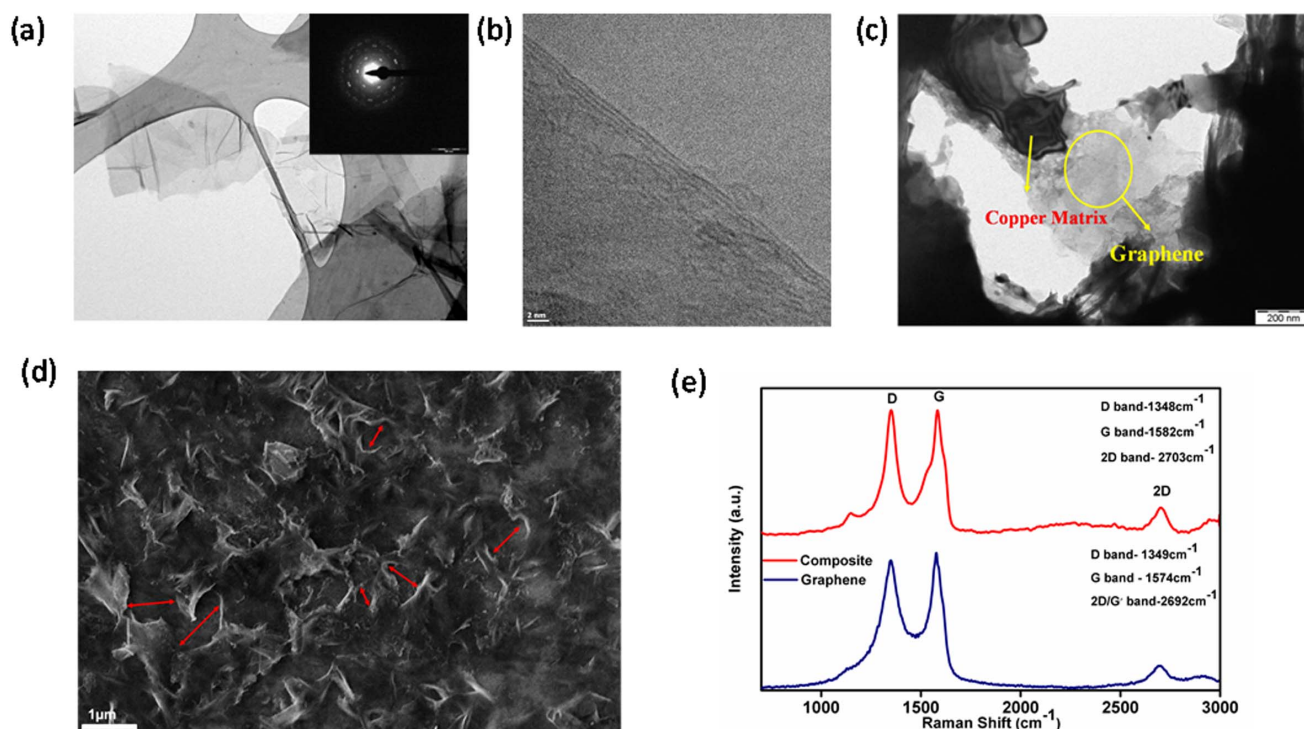


Figure 2 | (a) & (b) TEM images of Gr, (inset) Diffraction pattern (c) TEM and (d) FESEM images of Cu-Gr composite foil representing the presence and distribution of Gr in the matrix (e) Raman spectra for Gr and Cu-Gr composite foils.

The images clearly indicate the number of layers. The GO sheets were observed to be transparent and highly stable under the electron beam. The graphitic laminar structure can be observed from the electron diffraction as shown in the inset of Fig. 2 (a). The well-defined diffraction spots confirm the crystalline structure of Gr obtained by electrochemical exfoliation. GO used in the present process mainly consisted of 1–5 layers and were ~ 500 nm–1 μ m in diameter considering the graphene sheet to be in circular shape. Fourier transform infrared (FTIR) studies confirmed the presence of the O–H stretching mode (~ 3432 cm^{-1}), C=C (~ 1630 cm^{-1}), C–OH (~ 1382 cm^{-1}) and COOH (~ 1720 cm^{-1}) groups as shown in Fig. S2 (supporting information). Fig. 2(c) shows the TEM image of the twin-jet polished Cu-Gr composite confirming the presence of Gr in the Cu matrix, while the FESEM image (Fig. 2d) of the surface of the electropolished and etched Cu-Gr foil shows uniformly distributed graphene sheets in Cu matrix, which spread through the grain boundaries of Cu matrix. The distance (~ 800 nm–1.2 μ m) between the graphene sheets (marked by red arrows) is found to be comparable to that of the grain size of the matrix as shown in FIB etched Cu-Gr foils (Fig. 3(c) and Fig. S5(b)). X-Ray Diffraction (XRD) patterns for pure Cu foils and Cu-Gr foils prepared by DC and PRED are shown in Figure S1 (Supporting information). Similar patterns were observed for all the composite foils. Peaks corresponding to Gr/GO were not observed since the amount of GO incorporated into the composite is too small to be detected by XRD. Raman spectroscopy, a powerful tool to determine the presence of Gr, the number of layers, crystallinity, defects etc., confirmed the presence of Gr in Cu-Gr foils macroscopically. In the Raman spectra (Fig. 2e), composite foils with Gr as reinforcement have shown a D-Band at a wave number of 1348 cm^{-1} , and slight shift in the G-band (from 1574 to 1582 cm^{-1}) and 2D bands (from 2692 to 2703 cm^{-1}) from those observed for Gr. A slight increment in the intensity of the D-band compared to the G-band is observed in the composite foils, which may be due to the stresses formed in Gr and crumpling/folding of Gr in the matrix during co-deposition with Cu. It has been reported that in case of CNT reinforced composites, Raman bands

change their positions and intensities due to stresses and strains induced at the interface³³.

Figures 3a, b and c show the micrographs of Focussed Ion Beam (FIB) etched surface of the electropolished pure Cu foils prepared by PRED, Cu-Gr foils prepared by DC and PRED, respectively. PRED pure Cu has nearly uniform grain size of 1.3 ± 0.3 μ m (Fig. 3a & Fig. S5 (a)). PRED Cu-Gr also has exhibited uniform grain size with an average size of 1.2 ± 0.4 μ m (Fig. 3c & Fig. S5 (b)), while Cu-Gr composite foils prepared by application of DC resulted in grains with broader size distribution (Fig. 3b). Growth twins are also present in as-deposited pure Cu as well as composite foils. PRED is advantageous over DC electrodeposition because it offers to vary several key processing parameters including applied current, pulse duration and duty cycle that enables a smooth, highly dense, uniform deposit, while minimizing hydrogen embrittlement. This in turn improves the properties of the deposited material. The forward pulse restricts the mass transfer process and controls the grain size; whereas the reverse pulse minimizes the dendritic morphology and helps in the removal of extended Gr and loosely adsorbed Cu or Gr, in addition to removal of entrapped hydrogen during each pulse³⁴. Furthermore, the incorporation of Gr into the matrix is expected to be higher in PRED. In case of DC deposition, due to the continuous application of current, the deposition is rapid at the most active nucleation sites, and continuous incorporation of Gr along with the Cu deposition results in rough surface as well as formation of Gr clusters in the matrix. Our group has previously shown that use of PRED with controlled pulse parameters enables highly dense, smooth, highly textured (111) Cu foils with high hardness and good electrical conductivity³⁵.

The electrodeposited pure Cu and Cu-Gr foils were annealed at 300°C in argon atmosphere for 30 min in order to study the grain growth kinetics. The most interesting results have been achieved for the annealed Cu-Gr composite foils. Fig. 3 (d, e & f) show the micrographs of the annealed PRED-Cu, DC-Cu-Gr and PRED-Cu-Gr foils, respectively after etching the surface with FIB. Grain size in the pure Cu foil increased up to 10 microns upon annealing (Fig. 3d),

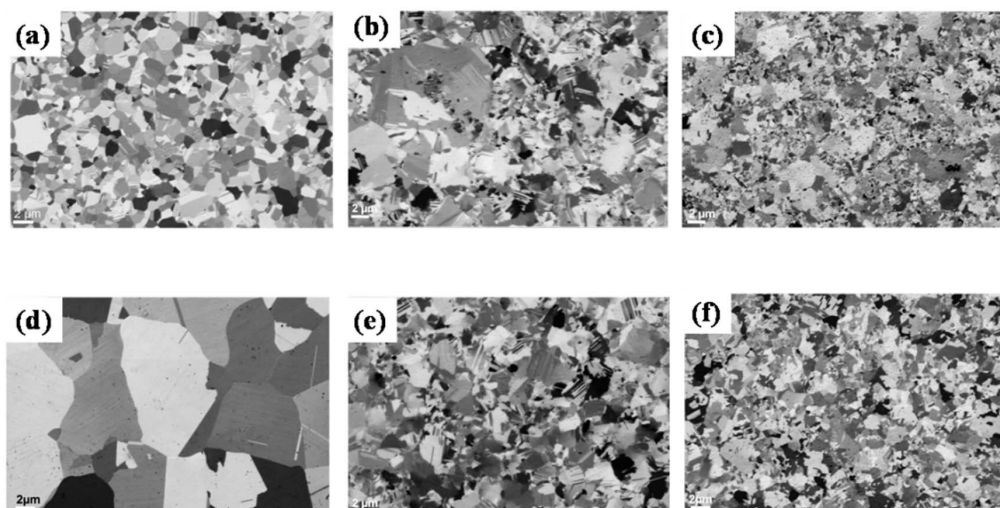


Figure 3 | (a), (b) & (c) FIB images of as-deposited and polished surface of PRED Pure Cu, DC Cu-Gr and PRED Cu-Gr. (d) (e) & (f) represent the annealed PRED Pure Cu, DC Cu-Gr, PRED Cu-Gr respectively.

whereas Cu-Gr foils have not shown any significant increase in the grain size (Fig. 3e & f) due to the presence of Gr as the second phase material at the grain boundary, which obstructs the motion of grain boundaries and thus retards the grain growth. It is well established that the morphology of the second phase plays a significant role in the grain growth kinetics. Needle-like structures as well as flake-like structures of the reinforcement material are found to be more effective in controlling the overall microstructural features of the composite^{36,37}. In addition to being a good reinforcement material, Gr with its sheet-like structure is expected to be a better grain growth inhibitor. It is clearly evident from the FESEM image of the surface of the electropolished Cu-Gr foil (Fig. 2d) that the Gr is distributed along the grain boundaries.

Hardness and elastic modulus of the Cu-Gr foils prepared by PRED and DC are evaluated by nanoindentation technique, using the method described by Oliver and Pharr^{38,39} with a Hysitron Triboindenter. The applied peak load was 2000 μN with a loading rate of 500 $\mu\text{N}/\text{sec}$, a Berkovich tip was used for the indentation. The load-displacement curves obtained during nanoindentation are shown in Figures 4 (a & b), and the corresponding hardness and modulus are shown in Fig. 4(c & d). Each hardness or elastic modulus datum point is an average of 25 indents performed under similar conditions. The hardness and the elastic modulus obtained for pure Cu synthesized by PR and DC electrodeposition are also shown in the figure 4(c & d) for comparison. Pure Cu foils exhibited hardness in the range of 1.4 – 1.6 GPa, while the composite foils have shown a hardness in the range of 2.1–2.5 GPa. This suggests that the inclusion of Gr substantially increases the hardness by 96% in these novel composites. In comparison to DC conditions, PR conditions have yielded higher hardness values for the composite foils because of the absence of agglomeration of graphene sheets and thereby resulting in uniform distribution of Gr throughout the matrix. The overall hardness of these composites have contributions from three factors, 1) finer grain size of the matrix, 2) presence of twins and 3) presence of Gr as a reinforcement. According to Hall-Petch relation, the grain size has to be in the range of 300 nm^{35,40} to achieve the high hardness >2 GPa in pure Cu prepared by electrodeposition. However, in the present study, a hardness of >2 GPa is achieved for Cu-Gr composite foils even with a large grain size of $\sim 1.2 \mu\text{m}$ clearly indicating the Gr role in enhancing the hardness. Since the grain size of the matrix is comparable in both the composites prepared by different processing parameters (DC and PRED), it is clear that, the presence of Gr causes the improvement in the hardness, whereas pure Cu foils of similar grain size are exhibiting much lower hardness. Although, the

presence of twin boundaries contribute in blocking the dislocation motion, the effect of twin boundaries is similar in both pure Cu and Cu-Gr foils. In addition, the -COOH and -OH groups attached to GO are expected to form covalent bonding between the Cu matrix and the graphene enabling efficient load transfer. Hwang et al.²⁵, have shown that the oxygen mediated bonding between copper and carbon enhances the bonding strength by a strong covalent bonding. Similar studies have also been reported for Cu-CNT composites^{41,42}. In addition, Park et al.⁴³, have also reported in their theoretical study that these functional groups predominantly form covalent bonding between Cu and CNT. As the FTIR spectrum (Fig. S2 Supporting information) in the present study shows the presence of -OH and -COOH functional groups on the surface, we assume the formation of covalent bonding between the matrix and the reinforced material in the present work. Uniform dispersion and spread of Gr throughout the matrix also arrests the grain growth during deposition and subsequently blocks the dislocation motion during deformation process. The decrement in the hardness of Cu-Gr composite films upon annealing is not significant, because of the retention of the microstructural features. Even though GO present near the surface of the film may undergo reduction during annealing, residual functional groups present in bulk of the Cu retain the interfacial bonding between Cu and GO. In contrast, as-deposited pure Cu foils contained larger grains due to absence of Gr and resulted in much lower hardness values compared to those of Cu-Gr foils and have shown drastic grain growth during annealing. However, against the expectations, the hardness for pure Cu foils did not decrease upon annealing (Figure 4c), probably due to the formation of annealing twins in addition to the growth twins, which are known to form in PRED, that compensate to the decrease in hardness due to grain-growth⁴⁴. Nanoindentation was also carried out on PRED Cu-Gr samples at different peak loads ranging from 1000 μN to 8000 μN and the data obtained for Hardness Vs. Peak load and Hardness Vs. Contact Depth are shown in Figures S3a & S3b (Supporting information). It is clear from these studies that the hardness was constant throughout and was not influenced by the peak load (contact depth).

Although modulus is independent of the microstructure, in case of composites, the values depend on the reinforced material, its distribution and the volume fraction in the matrix. It can be observed from Fig. 4 (d) that the modulus of the PRED Cu-Gr composite foils is higher, ranging between 127 – 137 GPa, compared to ~ 116 GPa for pure PRED Cu foils, which can be attributed to the presence of Gr. Interestingly, only a slight decrease in the modulus values was observed after annealing at 300°C for both pure Cu and composite

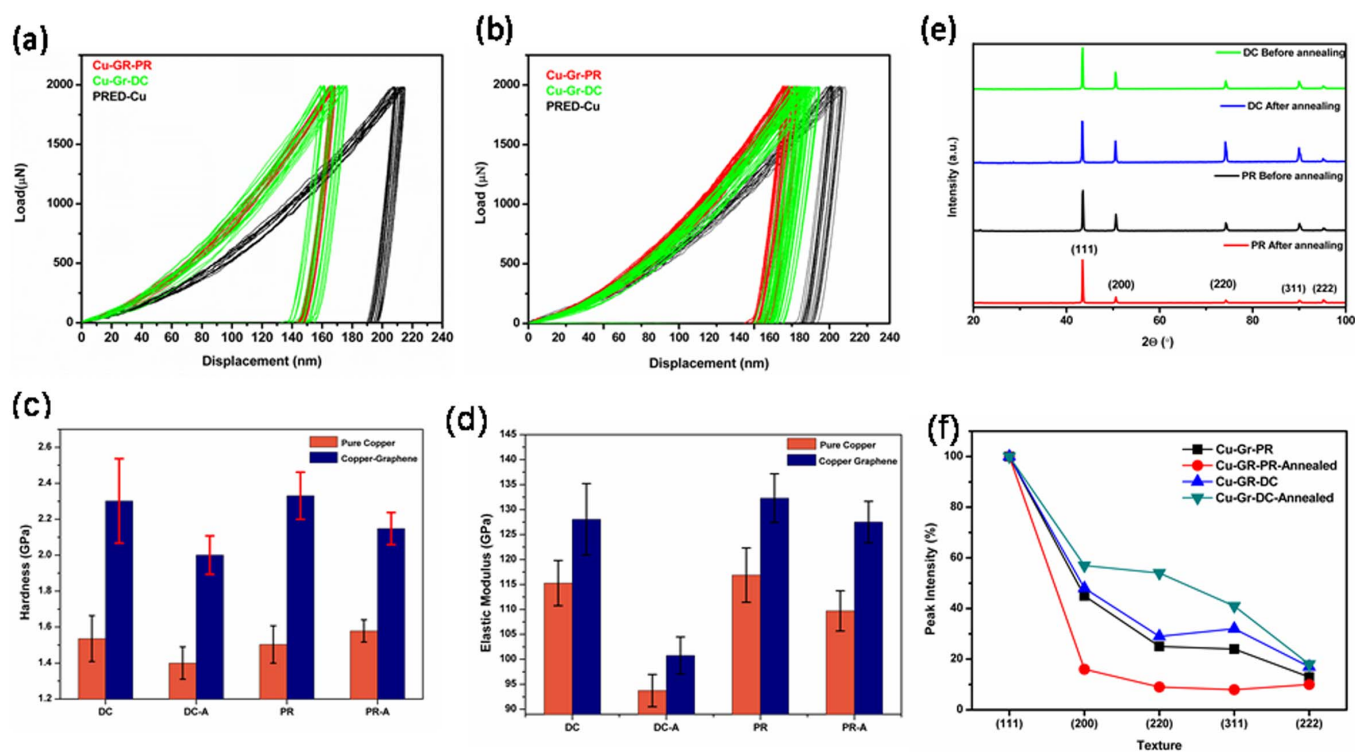


Figure 4 | Load displacement curves of (a) as deposited and (b) annealed PRED pure Cu, Cu-Gr composite foils (c) & (d) Plots exhibit the hardness and elastic modulus of as-deposited and annealed pure Cu and Cu-Gr composite foils prepared by DC and PRED (e) XRD patterns of the and (f) Intensities of crystallographic orientation calculated from XRD patterns.

foils prepared by PRED, while a large decrease is observed for the samples deposited using DC. The large decrease in modulus for DC samples during annealing could be due to the annihilation of residual stresses induced during DC process⁴⁵. It has also been reported by Xiang et al.⁴⁶, that annealing can reduce the residual stresses resulting in decrease of the modulus⁴⁷. Since PRED enables deposition of foils with very low residual stresses⁴⁸, only a slight decrease in the modulus is observed upon annealing (Fig. 4d). In addition, they have shown an increase in the (111) orientation upon annealing, which is common in pulse electrodeposited films⁴⁹. Many studies have shown that annealing can bring a preferential orientation of grains⁵⁰, which favours high modulus^{51,52}. Recently, we have also observed higher modulus for (111) textured pulse electrodeposited Cu foils compared to (100) and (101) oriented foils. Thus annealing induced (111) orientation in the present work (Fig. 4e & f) compensates, to some extent, the decrease in modulus that arises from residual stress release, and thus lesser decrease in the value of modulus compared to that of the DC deposited foils is observed.

Electrical resistivity of Cu-Gr composite foils was measured by four-point probe method. The resistivity of as-deposited PRED Cu-Gr composite foils is observed to be $\sim 3.4 \times 10^{-6} \Omega\text{-cm}$ and is decreased to $\sim 2.3 \times 10^{-6} \Omega\text{-cm}$ upon annealing at 300°C under argon atmosphere, for 30 min (Figure S4, Supporting information). The slight increment in the resistivity for as-deposited PRED Cu-Gr foils compared to that of pure Cu foils ($1.7 \times 10^{-6} \Omega\text{-cm}$) might be either due to the presence of poorly conducting GO incorporated into the matrix or due to the formation of small amount of Cu oxide during anodic pulse. Generally, upon annealing in inert atmosphere, stress relaxation leading to grain growth and removal of residual oxygen resulting in a decrease in the resistivity of the material. GO must be reacting with Cu to form Cu oxide and Gr, while Cu oxide being reduced to Cu during annealing²⁸. The resistivity values obtained are well in the range of the values reported for Cu-Gr and Cu-CNT composites^{28,31}.

Discussions

To conclude, Cu-Gr composite foils are synthesized, for the first time, by PRED technique by dispersing GO into the electrolyte in order to achieve superior mechanical properties, while exhibiting electrical conductivity in the same range as that of pure Cu. For comparative studies, composite foils are also deposited using DC method. Application of pulse reverse current has resulted in uniform distribution of Gr in the metal matrix. Nanoindentation studies showed that the PRED electrodeposited Cu-Gr composite foils have exhibited a high hardness of 2.2–2.5 GPa (increased by $\sim 96\%$ of that of pure Cu). The uniformity throughout the foils in terms of hardness was high for the PRED foils compared to that observed for the DC deposited foils. The elastic modulus of the foils prepared by PRED is ~ 137 GPa, which is $\sim 30\%$ higher than that for pure Cu foils. Annealing of PRED Cu-Gr foils have not shown considerable decrement in the hardness and modulus values indicating the promise of these foils, for several applications. The superior mechanical properties obtained as already mentioned, are mainly due to fine grain size of the Cu matrix and presence of Gr as reinforcement and its uniform distribution throughout the matrix. The uniformity in the microstructural features of these novel nanocomposites can be attributed to the feasibility to optimize several parameters including the applied current density, pulse ‘on’ and ‘off’ times both during the ‘forward pulse’ and the ‘reverse pulse’ unlike in DC deposition which allows variation of current density alone. Our present process is appropriate to prepare Cu-Gr composite foils with control over the mechanical and electrical properties, as it is a scalable low temperature process, economical and can be prepared on substrates with complex shapes with good reproducibility.

Methods

Synthesis of Cu-Gr composite foils. GO was synthesized by electrochemical exfoliation of graphite in an aqueous electrolyte consisting of HNO_3 . GO nanosheets were washed thoroughly by ultrasonication and centrifugation followed by drying at 60°C. During the electrochemical exfoliation, the GO was prepared with the required



functional groups attached to its surface; therefore no further functionalization was required to achieve dispersion into the electrolyte. Cu-Gr composite foils are synthesized in an electrolytic bath consisting of 250 g/L Copper Sulphate, H_2SO_4 was added to maintain the pH at ~ 1 . In order to avoid the agglomeration of Gr sheets in the electrolyte during the deposition, a polymeric surfactant like PAA5000 (25 ppm for 0.5 g/L of Gr) was added. Other surfactants like SDS, CTAB, etc., have resulted in formation of powdery deposit. GO content dispersed in the electrolyte was varied between 0.1–1 g/L. However, the optimum concentration was found to be 0.5 gm/L in order to achieve Cu-Gr foils with high hardness, less agglomeration of Gr in matrix and good reproducibility. Therefore the present investigations were performed using the Gr concentration as 0.5 gm/L in the electrolyte. Bath temperature was maintained between 15–20°C. Electrodeposition was done with a two electrode system by using a Dynatronix pulse power supply (DuPR10-3-6) with an electrolytic Cu sheet (99.99%) as anode and titanium plate as cathode (Figure 1). In order to easily peel off the deposited composite foil from the titanium substrate, pure Cu film of 2 μm was deposited as a seed layer prior to the composite deposition. Fig. 1 (b & c) shows the schematic representation, explaining the pulse pattern and the deposition process during DC and PRED. GO was dispersed in the electrolyte by ultrasonication at room temperature for 3 hrs. prior to deposition. The electrodeposition was carried out under magnetic stirring. DC electrodeposition was done by applying a current density of 0.025 A/cm². In case of PRED, the current densities for the forward and reverse pulses were optimized by performing the depositions in the range of 0.05–0.2 A/cm² and 0.005–0.015 A/cm², respectively. The forward pulse on (T_{on}) time is in the range of 15–50 ms, T_{off} is in the range of 50–100 ms and T_{Ron} and T_{Roff} are in the range of 1–10 ms. Adoption of both PRED and DC methods resulted in foils of ~ 30 μm thickness. The electrodeposited Cu and Cu-Gr foils were annealed at 300°C for 30 min under argon atmosphere using tubular furnace.

Characterization techniques used for Cu-Gr composites. The surface morphology, grain size and the distribution of Gr in the composite foils were examined by Field Emission Scanning Electron Microscope (Carl Zeiss Ultra 55), Focussed Ion Beam (Carl Zeiss Neon 40) and Transmission Electron Microscope (FEI Tecnai G² 200 KV). Crystallographic orientation of the composite was characterized by XRD (D8 BRUKER D8 ADVANCE X-ray diffractometer). Presence of Gr in the Cu-Gr foils was confirmed by Raman spectroscopy (LabRAM HR800-JOBINYUON), where the laser source was Ar-ion laser (514 nm). Mechanical and electrical properties were obtained by nanoindentation (Hysitron Triboindenter T1950) and 4-probe resistivity (Mitsubishi- Loresta Series) techniques respectively.

- Geim, A. K. & Novoselov, K. S. The rise of graphene. *Nat Mater* **6**, 183–191 (2007).
- Huang, X., Qi, X., Boey, F. & Zhang, H. Graphene-based composites. *Chem Soc Rev* **41**, 666–686 (2012).
- Lee, C., Wei, X., Kysar, J. W. & Hone, J. Measurement of the elastic properties and intrinsic strength of monolayer graphene. *Science* **321**, 385–388 (2008).
- Novoselov, K. S. *et al.* Electric field effect in atomically thin carbon films. *Science* **306**, 666–669 (2004).
- Balandin, A. A. Thermal properties of graphene and nanostructured carbon materials. *Nat Mater* **10**, 569–581 (2011).
- Su, C. Y., Lu, A. Y., Xu, Y., Chen, F. R., Khlobystov, A. N. & Li, L. J. High-quality thin graphene films from fast electrochemical exfoliation. *ACS Nano* **5**, 2332–2339 (2011).
- Park, S. & Ruoff, R. S. Chemical methods for the production of graphenes. *Nat Nanotechnol* **4**, 217–225 (2009).
- Upadhyaya, A. & Upadhyaya, G. S. Sintering of copper-alumina composites through blending and mechanical alloying powder metallurgy routes. *Mater Des* **16**, 41–45 (1995).
- Chrysanthou, A. & Erbaccio, G. Production of copper-matrix composites by in situ processing. *J Mater Sci* **30**, 6339–6344 (1995).
- Hu, Y., Shenderova, O. A., Hu, Z., Padgett, C. W. & Brenner, D. W. Carbon nanostructures for advanced composites. *Rep Prog Phys* **69**, 1847–1895 (2006).
- Dresselhaus, M. S., Dresselhaus, G., Charlier, J. C. & Hernandez, E. Electronic, thermal and mechanical properties of carbon nanotubes. *Phil Trans R Soc Lond A* **362**, 2065–2098 (2004).
- Mendoza, M. E., Solórzano, I. G. & Brocchi, E. A. Mechanical and electrical characterization of Cu-2 wt.% SWCNT nanocomposites synthesized by in situ reduction. *Mater Sci Eng A* **544**, 21–26 (2012).
- Chai, G., Sun, Y., Sun, J. J. & Chen, Q. Mechanical properties of carbon nanotube – copper nanocomposites. *J Micromech Microeng* **035013**, 1–4 (2008).
- Bakshi, S. R., Lahiri, D. & Agarwal, A. Carbon nanotube reinforced metal matrix composites – a review. *Int Mater Rev* **55**, 41–64 (2010).
- Pfautsch, E. Challenges in commercializing carbon nanotube composites. *WISE Intern* **1**–43 (2007).
- Rafiee, M. A., Rafiee, J., Wang, Z., Song, H., Yu, Z.-Z. & Koratkar, N. Enhanced mechanical properties of nanocomposites at low graphene content. *ACS Nano* **3**, 3884–3890 (2009).
- Lee, D. *et al.* Enhanced mechanical properties of epoxy nanocomposites by mixing noncovalently functionalized boron nitride nanoflakes. *Small* **9**, 2602–2610 (2013).
- Song, S. H. *et al.* Enhanced thermal conductivity of epoxy-graphene composites by using non-oxidized graphene flakes with non-covalent functionalization. *Adv Mater* **25**, 732–737 (2013).
- Fan, W., Zhang, C., Tjui, W. W. & Liu, T. Fabrication of electrically conductive graphene/polystyrene composites via a combination of latex and layer-by-layer assembly approaches. *J Mater Res* **28**, 611–619 (2013).
- S. Walker, L., Marotto, V. R., Rafiee, M. A., Koratkar, N. & Corra, E. L. Toughening in graphene ceramic composites. *ACS Nano* **5**, 3182–3190 (2011).
- Wang, J., Li, Z., Fan, G., Pan, H., Chen, Z. & Zhang, D. Reinforcement with graphene nanosheets in aluminum matrix composites. *Scripta Mater* **66**, 594–597 (2012).
- Bartolucci, S. F. *et al.* Graphene – aluminum nanocomposites. *Mater Sci Eng A* **528**, 7933–7937 (2011).
- Chen, L.-Y. *et al.* Novel nanoprocessing route for bulk graphene nanoplatelets reinforced metal matrix nanocomposites. *Scripta Mater* **67**, 29–32 (2012).
- Kuang, D., Xu, L., Liu, L. & Hu, W. Graphene-nickel composites. *Appl Surf Sci* **273**, 484–490 (2013).
- Hwang, J. *et al.* Enhanced mechanical properties of graphene/copper nanocomposites using a molecular-level mixing process. *Adv Mater* DOI: **10.1002/adma.201302495**, (2013).
- Koltsova, T. S. *et al.* New hybrid copper composite materials based on carbon nanostructures. *J Mater Sci Eng B* **2**, 240–246 (2012).
- Jagannadham, K. Thermal conductivity of copper-graphene composite films synthesized by electrochemical deposition with exfoliated graphene platelets. *Metall Mater Trans B* **43B**, 316–324 (2012).
- Kasichainula, J. Electrical conductivity of copper – graphene composite films synthesized by electrochemical deposition with exfoliated graphene platelets. *J Vac Sci Technol B: Microelectron Nanometr Struct* **30**, 03 D109 (2012).
- Kim, Y. *et al.* Strengthening effect of single-atomic-layer graphene in metal-graphene nanolayered composites. *Nat Commun* **4**:2114, DOI: **10.1038/ncomms3114**, (2013).
- Low, C. T. J., Wills, R. G. A. & Walsh, F. C. Electrodeposition of composite coatings containing nanoparticles in a metal deposit. *Surf Coat Tech* **201**, 371–383 (2006).
- Subramaniam, C. *et al.* One hundred fold increase in current carrying capacity in a carbon nanotube –copper composite. *Nat Commun* **4**:2202, DOI: **10.1038/ncomms3202**, (2013).
- Niu, Y. *et al.* Large area orientation films based on graphene oxide self-assembly and low-temperature thermal reduction. *Appl Phys Lett* **101**, 181903 (2012).
- Coopera, C. A., Younga, R. J. & Halsallb, M. Investigation into the deformation of carbon nanotubes and their composites through the use of raman spectroscopy. *Composites A* **32**, 401–411 (2001).
- Chandrasekar, M. S. & Pushpavanam, M. Pulse and pulse reverse plating – Conceptual, advantages and applications. *Electrochim Acta* **53**, 3313–3322 (2008).
- Sarada, B. V., Pavithra, C. L. P., Ramakrishna, M., Rao, T. N. & Sundararajan, G. Highly (111) Textured copper foils with high hardness and high electrical conductivity by pulse reverse electrodeposition. *Electrochem Solid-State Lett* **13**, D40–D42 (2010).
- Chang, K., Feng, W. & Chen, L.-Q. Effect of second-phase particle morphology on grain growth kinetics. *Acta Mater* **57**, 5229–5236 (2009).
- Ohji, G.-JZaT. Effect of BN content on elastic modulus and bending strength of SiC-BN in situ composites. *J Mater Res* **15**, 1876–1880 (2000).
- Oliver, W. C. & Pharr, G. M. An improved techniques for determining hardness and elastic modulus using load and displacement sensing indentation experiments. *J Mater Res* **7**, 1564–1583 (1992).
- Oliver, W. C. & Pharr, G. M. Measurement of hardness and elastic modulus by instrumented indentation: Advances in understanding and refinements to methodology. *J Mater Res* **19**, 3–20 (2004).
- Hakamada, M. *et al.* Relationship between hardness and grain size in electrodeposited copper films. *Mater Sci Eng: A* **457**, 120–126 (2007).
- Lavanya, A. & Klaus-Juergen, W. Carbon nanotube composites for electronic packaging applications: A Review. *J Nanotech* **2013**, 6 (2013).
- Kim, K. T., Cha, S. I., Gemming, T., Eckert, J. & Hong, S. H. The role of interfacial oxygen atoms in the enhanced mechanical properties of carbon-nanotube-reinforced metal matrix nanocomposites. *Small* **4**, 1936–1940 (2008).
- Park, M., Kim, B.-H., Kim, S., Han, D.-S., Kim, G. & Lee, K.-R. Improved binding between copper and carbon nanotubes in a composite using oxygen-containing functional groups. *Carbon* **49**, 811–818 (2011).
- Xu, D., Kwan, W. L., Chen, K., Zhang, X. & Vidvuds Ozoliņš, Tu K. N. Nanotwin formation in copper thin films by stress/strain relaxation in pulse electrodeposition. *Appl Phys Lett* **91**, 254105 (2007).
- Alanazi, N. M., El-Sherik, A. M., Alamar, S. H. & Shen, S. Influence of residual stresses on corrosion and wear behavior of electrodeposited nanocrystalline cobalt-phosphorus coatings. *Int J Electrochem Sci* **8**, 10350–10358 (2013).
- Xiang, Y., Tsui, T. Y. & Vlaskak, J. J. The mechanical properties of freestanding electroplated Cu thin films. *J Mater Res* **21**, 1607–1618 (2006).
- Okoro, C. *et al.* Influence of annealing conditions on the mechanical and microstructural behavior of electroplated Cu-TSV. *J Micromech Microeng* **20**, 1–6 (2010).
- Guan, S. & Nelson, B. J. Pulse-Reverse electrodeposited nanograined CoNiP thin films and microarrays for MEMS actuators. *J Electrochem Soc* **152**, C190–C195 (2005).
- Kwon, D., Park, H., Ghosh, S., Lee, C., Jeon, H. T. & Lee, J. G. Recrystallization of the copper films deposited by pulsed electroplating on ECR plasma-cleaned copper seed layers. *J Korean Phys Soc* **44**, 1108–1112 (2004).



50. Fong, D. D. Stresses in Cu thin films and Ag/Ni multilayers. Thesis. In: *Engineering & Applied Sciences*. Harvard University, (Cambridge, Massachusetts) (2001).
51. Srikanth, N., Premkumar, J., Sivakumar, M., Wong, Y. M. & III, C. J. V. Effect of wire purity on copper wire bonding. In: *9th Electronics Packaging Technology Conference*. Singapore, IEEE (2007).
52. Xiang, Y., Chen, X. & Vlassak, J. J. The Mechanical properties of electroplated Cu thin films measured by means of the bulge test technique. In: *Mater. Res. Soc. Symp. Proc.* Warrendale, PA (2002).

Acknowledgments

This work was supported by Nanomission Programme of Department of Science and Technology. The authors would like to thank Varam Sreedevi, SEST, University of Hyderabad for helping with Nanoindentation studies, and Mr L. Venkatesh, CMCT, ARCI for FIB imaging.

Author contributions

C.L.P.P., B.V.S.: design and study of experiments and research. K.V.R. contributed to the

interpretation of nanoindentation data and mechanical properties. T.N.R. and G.S. contributed to the discussions of the data. All authors contributed equally to the interpretation of the data and provided significant effort to the final manuscript. All authors reviewed the manuscript.

Additional information

Supplementary information accompanies this paper at <http://www.nature.com/scientificreports>

Competing financial interests: The authors declare no competing financial interests.

How to cite this article: Pavithra, C.L.P., Sarada, B.V., Rajulapati, K.V., Rao, T.N. & Sundararajan, G. A New Electrochemical Approach for the Synthesis of Copper-Graphene Nanocomposite Foils with High Hardness. *Sci. Rep.* 4, 4049; DOI:10.1038/srep04049 (2014).



This work is licensed under a Creative Commons Attribution-NonCommercial-NoDerivs 3.0 Unported license. To view a copy of this license, visit <http://creativecommons.org/licenses/by-nc-nd/3.0>